

Electronic Supplementary Information

Sulfur-modified porous covalent organic polymers as bifunctional materials for efficient fluorescence detection and fast removal of heavy metal ions

Jin Li¹, Shitao Wang^{1*}, Xiaohua Cao², Huanan Huang², Dapeng Cao^{1*}

¹ *Beijing Advanced Innovation Center for Soft Matter Science and Engineering, State Key Laboratory of Organic-Inorganic Composites, Beijing University of Chemical Technology, Beijing 100029, China.*

² *School of Chemistry and Environmental Engineering, Jiujiang University, Jiujiang 222005, China.*

Correspondence to: stwang@mail.buct.edu.cn; caodp@mail.buct.edu.cn

Table of Contents

Section 1. Methods	S3
Section 2. Materials and Synthetic Procedures.....	S5
Section 3. Supporting Tables and Figures	S9
Section 4. Supporting References	S24

Section 1. Methods

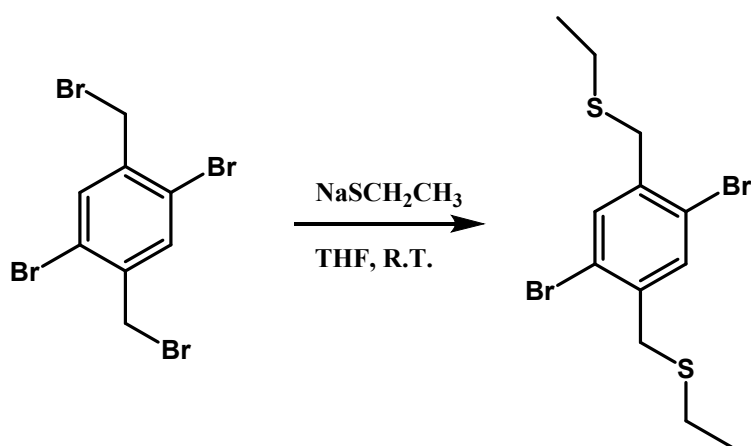
¹H Nuclear Magnetic Resonance (NMR, 400 MHz) spectral data were obtained on the Bruker Avance spectrometers with tetramethylsilane (TMS) as internal reference and peak multiplicity was reported as follows: s, singlet; d, doublet; t, triplet. Powder X-ray diffraction (PXRD) patterns were carried out with Ultima IV with Cu-K_{α1} radiation ($\lambda = 1.5406 \text{ \AA}$) at the rate of 5°/min. Thermo gravimetric analysis (TGA) data was obtained on a TGA/DSC1 1600 instrument, with a heating rate of 10 °C min⁻¹ under flowing N₂. FTIR spectroscopy was performed on an VERTEX 70v (Bruker) instrument with the wave range of 4000-400 cm⁻¹. Scanning electron microscope (SEM) images were obtained on a SIGMA 500 SEM instrument. Transmission electron microscope (TEM) characterizations were conducted using a JEN 1400 with an accelerating voltage of 200 KV. Fluorescence spectra were recorded at room temperature using a Hitachi F-7000 spectrophotometer with a PMT voltage of 550 V and a scan speed of 1200 nm/min; If no special instructions, the slit width for both excitation and emission was 5 nm. The time-dependent fluorescence spectra recorded for COPs dispersed in ethanol indicated that COPs does not show any photo-bleaching. N₂ Adsorption: N₂ adsorption/desorption isotherms at 77 K were measured by a JWGB SCI. & TECH. JW-BK200. The samples were degassed at 200 °C for 10 h. Pore size distribution data were calculated from the N₂ sorption isotherms based on the BJH Adsorption model in the JWGB SCI. & TECH. JW-BK200 software package. The concentrations of Hg²⁺ during all the experiments were detected by inductively coupled plasma-optical emission spectroscopy (ICP-OES) and inductively coupled plasma-mass spectrometry (ICP-MS) for extra low concentrations. All the adsorption experiments were performed at ambient conditions. X-ray photoelectron spectroscopy (XPS)

measurements were performed on a ULVAC-PHI PHI5000 Versaprobe III, using non-monochromatic Al K α X-rays as the excitation source and choosing C 1s (284.8 eV) as the reference line.

Stock solutions (0.01 M) of the nitrate salts of Hg²⁺, K⁺, Ag⁺, Mg²⁺, Ba²⁺, Pb²⁺, Cu²⁺, Fe³⁺, Co²⁺, Ni²⁺, Zn²⁺, Cr³⁺ and Cd²⁺ were prepared in deionized water; and the stock solutions (0.1 M) of S²⁻ was prepared in deionized water using Na₂S. Stock solution of COPs (2 mg / 10 mL) was prepared by dispersion of COPS in ethanol.

Section 2. Materials and Synthetic Procedures

All reagents, unless otherwise stated, were obtained from commercial sources (J&K, Macklin, and Innochem) and were used without further purification.



Scheme S1 Synthetic route of the DB-S

Synthesis of DB-S: DB-S was synthesized according to previous literature,¹ To a Schlenk tube were added 1,4-dibromo-2,5-bis(bromomethyl)benzene (0.50 g, 1.18 mmol), THF(20 mL) under nitrogen. The mixture was cooled to 0 °C using ice bath. Sodium ethanethiolate (300 mg, 3.54 mmol) was added. The suspension was stirred at room temperature for 2.5 h. The reaction mixture was poured into H₂O (150 mL) and the product was extracted with dichloromethane (3 × 75 mL). The organic extracts were combined, dried over anhydrous Na₂SO₄, and concentrated to give the product as a grey solid: ¹H NMR (400 MHz, 298 K, CDCl₃, TMS) δ= 7.567 (s, 2H), 3.774 (s, 4H), 2.532 (q, J = 7.4 Hz, 4H), 1.273 (t, J = 7.4 Hz, 6H).

Synthesis of ZIF-8: zinc nitrate tetrahydrate (0.261 g, 1 mmol) and 2-methylimidazole (0.657 g, 8 mmol) were dissolved in 20 mL of methanol, respectively, and then mixed and stirred for 24 h. The product was collected by filter and washed with pure methanol for three times, then dry overnight.

Synthesis of COPs: The synthesis of COPs was carried out by Yamamoto reaction, using the two monomers of TBB and the derivatives of DB, DB-S. The specific synthesis methods are as follows. 1,5-Cyclooctadiene (COD, 0.505 mL, 3.96 mmol) was added to a solution of bis(1,5-cyclooctadiene)nickel(0) (Ni(COD)₂, 1.1250 g, 4.09 mmol), and 2,2'-bipyridyl (0.6400 g, 4.09 mmol) in dry dimethylformamide (DMF) (65 mL). The mixture was stirred until completely dissolved. TBB and DB or DB-S were subsequently added to the resulting purple solution in a ratio of 2:3, and the amounts of the two monomers are 0.314 vs 0.471 mmol. The reaction vessel was heated at 80° C overnight under a argon atmosphere. The above reaction is carried out in a glove box. After cooling to room temperature, concentrated HCl was added to the deep purple suspension, until the solution turns cyan and flocculent matter is observed. After filtration, the residue was washed by CH₂Cl₂(5×15 mL), tetrahydrofuran (THF) (5×15 mL) and H₂O (5×15 mL), respectively, and dried in a vacuum oven at 140°C for 10 h. The dried sample, named as COP-108, COP-108-S was placed in containers and stored in a desiccator.

For the sensing (sensitivity and selectivity) tests, 1.8 ml of the stock solution of COPs was added to a quartz cuvette. The fluorescence spectra were recorded immediately after an appropriate aliquot of the stock solution of metal ions was added (0.2 mL). The shape of the emission spectra was not changed upon the addition of the stock solutions of metal ions. The fluorescence competitive experiment is to add an appropriate amount of Hg²⁺ in the presence of other metal ions. The fluorescence titrations were carried out via gradually adding the stock solution of Hg²⁺ in an incremental fashion.

Hg²⁺ sorption isotherms. The equilibrium adsorption of Hg²⁺ on the polymers was performed by mixing 10 mg of the polymers with 30 mL of Hg²⁺ aqueous solution, the initial concentration ranges of Hg²⁺ from 50 to 1000 ppm, the pH range of the solution is 3-6. The adsorption was performed at 298 K with 3 h so that the adsorption reached equilibrium. The supernatant was analyzed using ICP analysis to determine the remaining Hg²⁺ concentration.

$$q_e = (C_0 - C_e)V/W \quad (1)$$

where q_e (mg/g) is the equilibrium capacity, C_0 (mg/L) and C_e (mg/L) are the initial and equilibrium concentration, respectively, V is the volume of the solution (L) and W is the mass of the polymers (mg).²

Hg²⁺ sorption kinetics. A certain concentration of Hg²⁺ solution (PH=6) and a certain amount of adsorbent were added to an Erlenmeyer flask with a magnetic stir bar. The mixture was stirred at room temperature for 3 h. At appropriate time intervals, the aliquots (3 mL) were taken from the mixture, and the adsorbents were separated by syringe filter (0.22 μm membrane filter). The Hg²⁺ concentration in the resulting solutions were analyzed by ICP-OES. The percentage removal of Hg²⁺ was calculated as follows²:

$$\text{Removal percentage (\%)} = (C_0 - C_t) / C_0 \times 100 \quad (2)$$

General procedure for recycling.

Fluorescence: 50 mg COP-108-S and 250 ml ethanol were added into a 500 ml beaker. After the mixture was fully ultra-sonicated for dispersion, an appropriate amount of 0.01 M of Hg²⁺ aqueous solution was added (the Hg²⁺ concentration in the resulted mixture was 1.0 x 10⁻³ M). The fluorescence emission spectrum was measured before and after adding Hg²⁺, respectively. For recycle use, the mixture was then filtrated through a filter paper and washed with water. The COP

sample was stirred in 50 ml of Na₂S solution (0.1 M) for 30 min, filtered and washed with water. The regenerated COP-108-S was used for next fluorescent measurement cycle.

Adsorption: COP-108-S (200 mg) was added to conical flask (250 ml) containing Hg²⁺ aqueous solution (100 ml, 18.13 ppm). The mixtures were stirred at room temperature for 3 h and filtrated through a filter paper and washed with water. The COP sample was collected and stirred in 50 ml Na₂S solution (0.1 M) for 30 min, then filtered and washed with water. The regenerated COP-108-S was used for next cycle.

Section 3. Supporting Tables and Figures

Table S1 Porosity properties of COP-108 and COP-108-S.

Materials	BET (m ² /g)	Pore volume (cm ³ /g) ^a	Pore size (nm)
COP-108	922.934	0.714	2.0~4.0
COP-108-S	102.608	0.137	2.0~5.0

^a Determined at P/P₀=0.99.

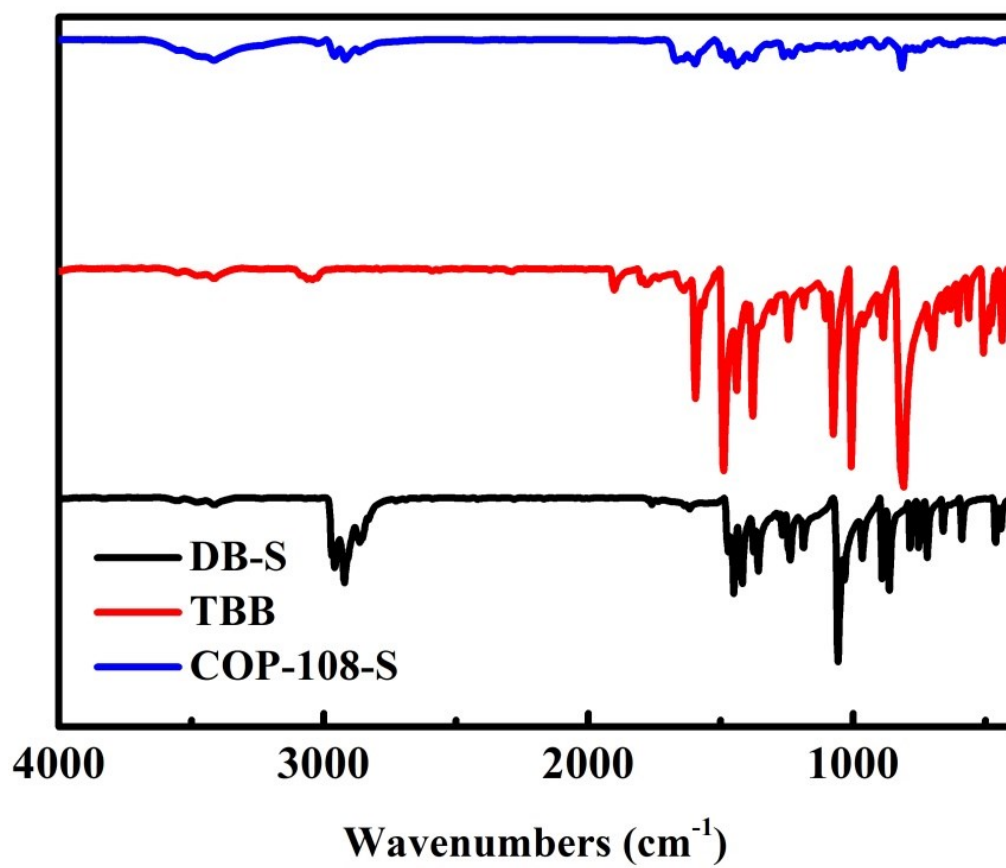


Figure S1. FT-IR spectra of the DB (black), TBB (red) and the COP-108-S (blue) from 400-4000 cm⁻¹.

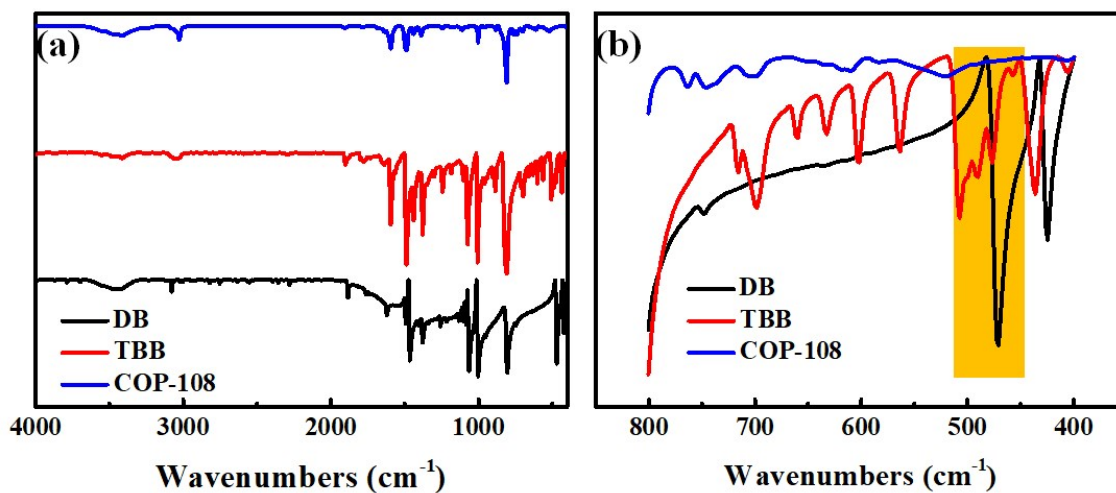


Figure S2. FT-IR spectra of the DB (black), TBB (red) and the COP-108 (blue) from 400-4000 cm⁻¹ (a) and 400-800 cm⁻¹(b). The characteristic absorption bands for Carbon-Bromine are highlighted via yellow region (see the right panel), clearly showing the lack of bromine in the COP-108 and indicating the formation of the polymeric COP-108 structure.

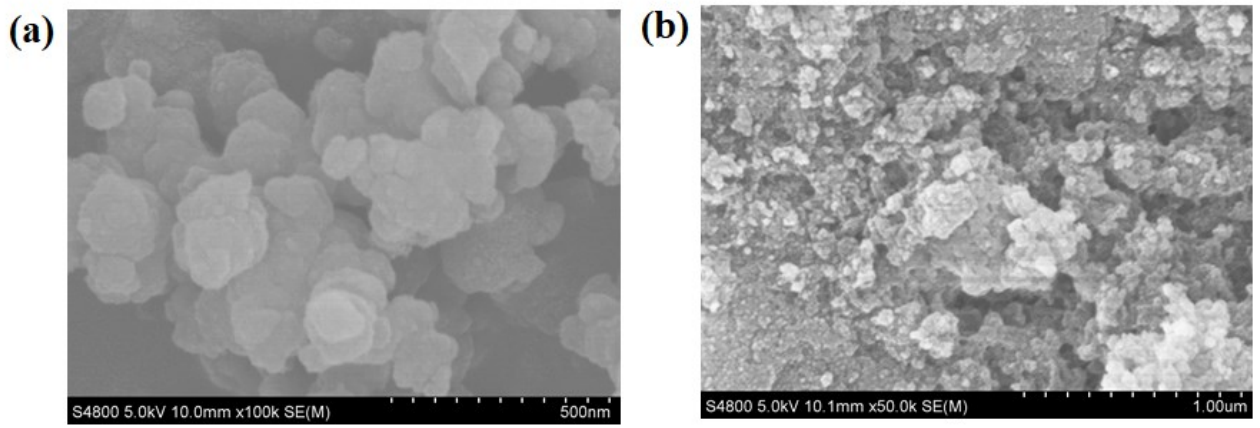


Figure S3. (a) SEM images of COP-108. (b) SEM images of COP-108-S.

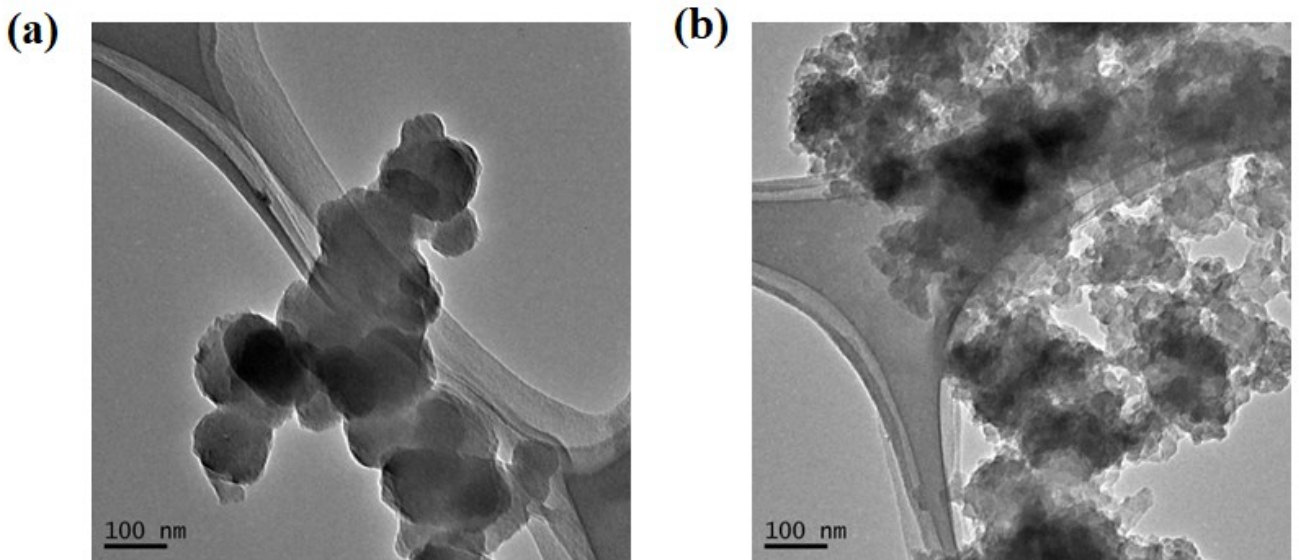


Figure S4. (a) TEM images of COP-108. (b) TEM images of COP-108-S.

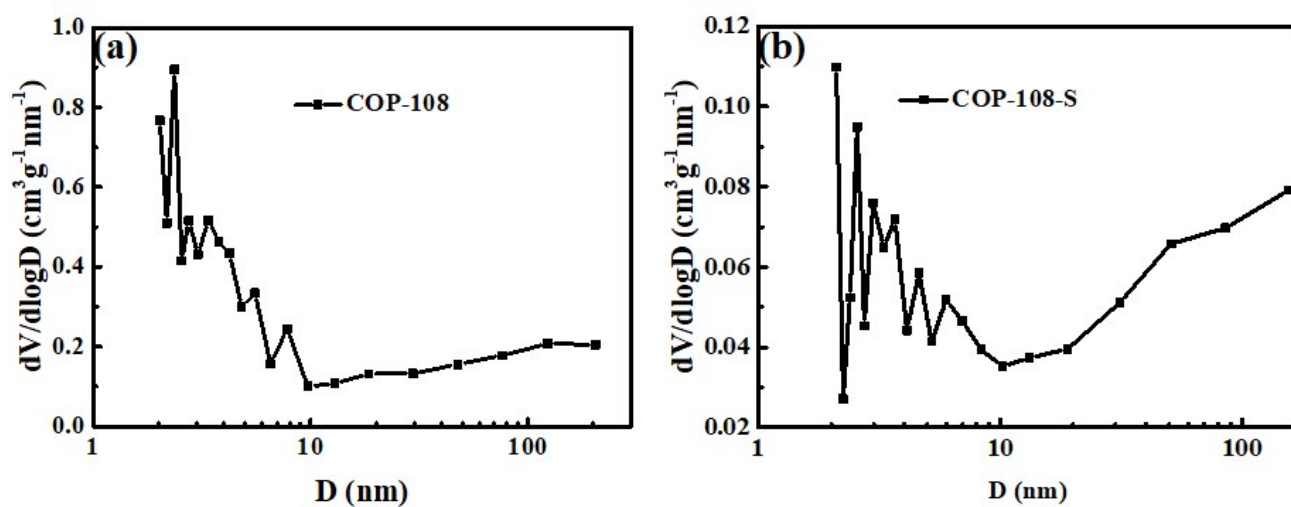


Figure S5. Barrett-Joyner-Halenda (BJH) pore size distributions of products by incremental pore volume. (a) COP-108, (b) COP-108-S.

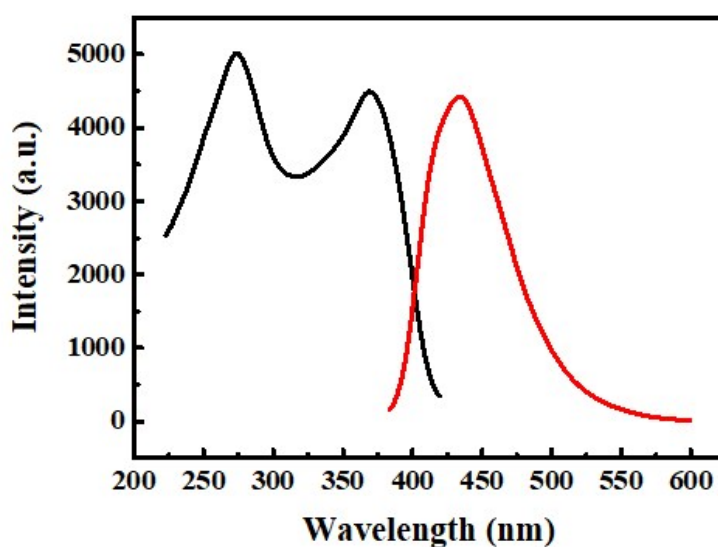


Figure S6. The solid-state excitation spectrum (black) and solid-state fluorescence emission spectrum (red) of COP-108, which exhibits an enhanced fluorescence emission with the maximum peak at 434 nm (excited at 372 nm).

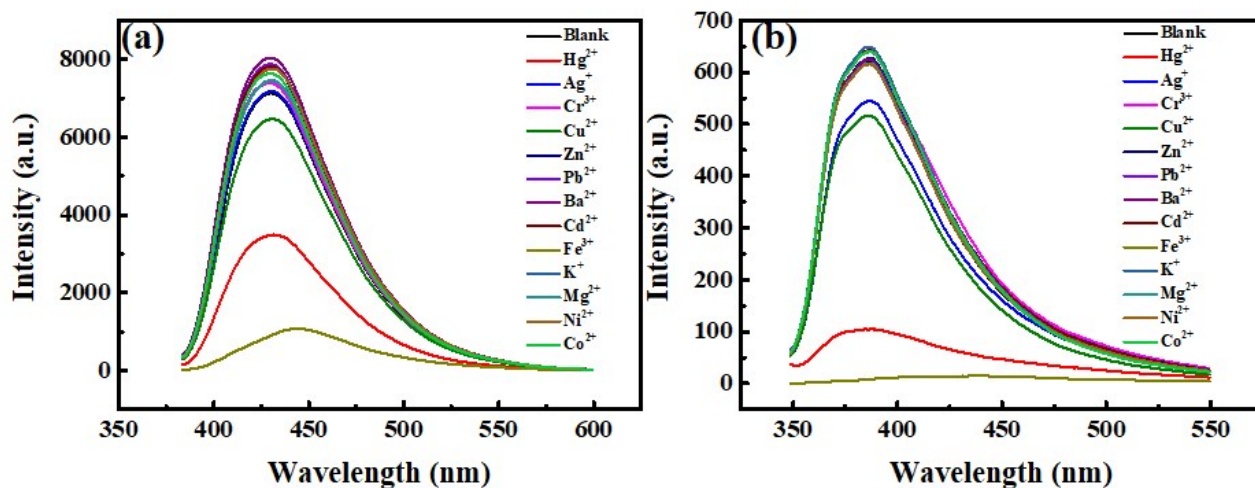


Figure S7. Fluorescence emission spectrum of materials dispersion with a concentration of 2 mg / 10 ml to detect various metal ions. (a) COP-108. (b) COP-108-S.

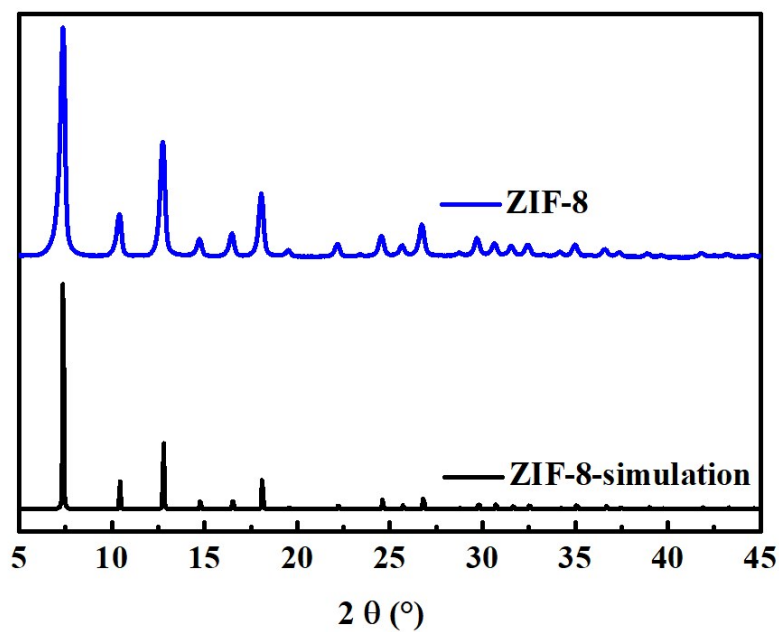


Figure S8. Powder XRD patterns of ZIF-8.

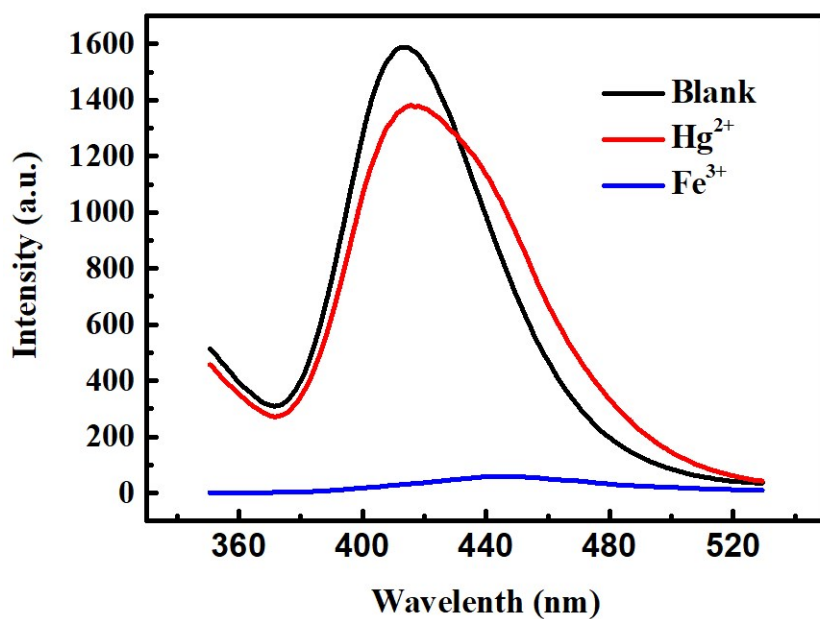


Figure S9. Fluorescence emission spectrum of the ZIF-8 interacting with different metal ions in 1×10^{-3} M DMF solution of $M(\text{NO}_3)_x$, where the widths of the excitation slit are 5 nm and emission slit is 10 nm for the ZIF-8.

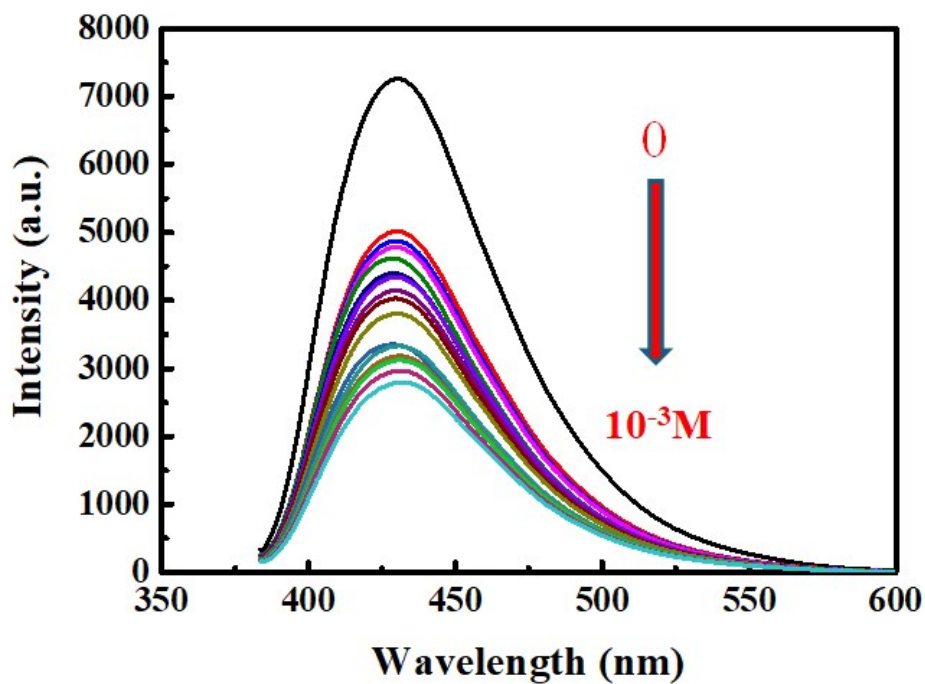


Figure S10. Fluorescence emission spectrum of the COP-108 in EtOH solutions containing $\text{Hg}(\text{NO}_3)_2$ of different concentrations. From top to bottom, the Hg^{2+} concentrations are from 0 to 10^{-3} M.

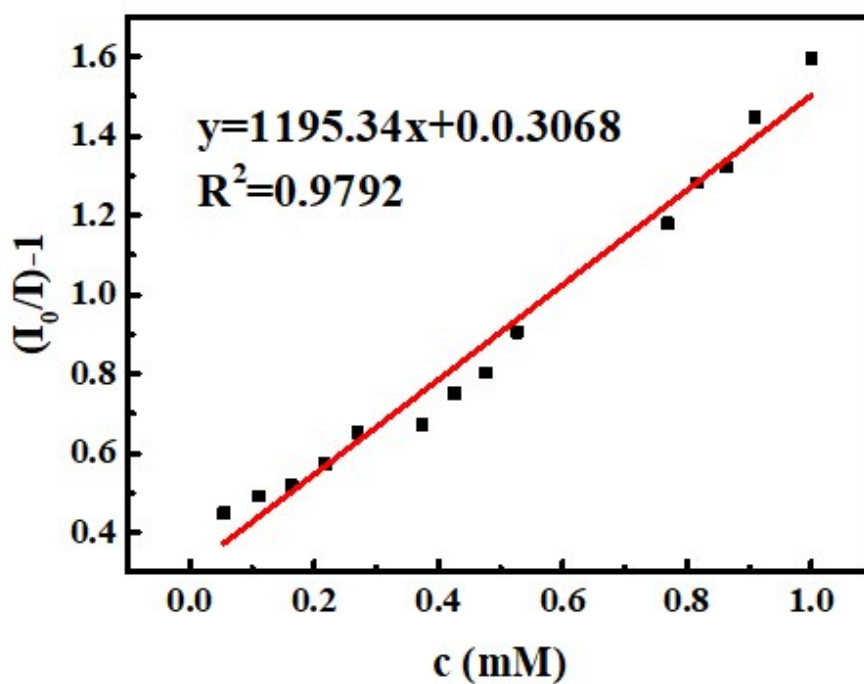


Figure S11. Stern-Volmer plots of COP-108 for Hg^{2+} .

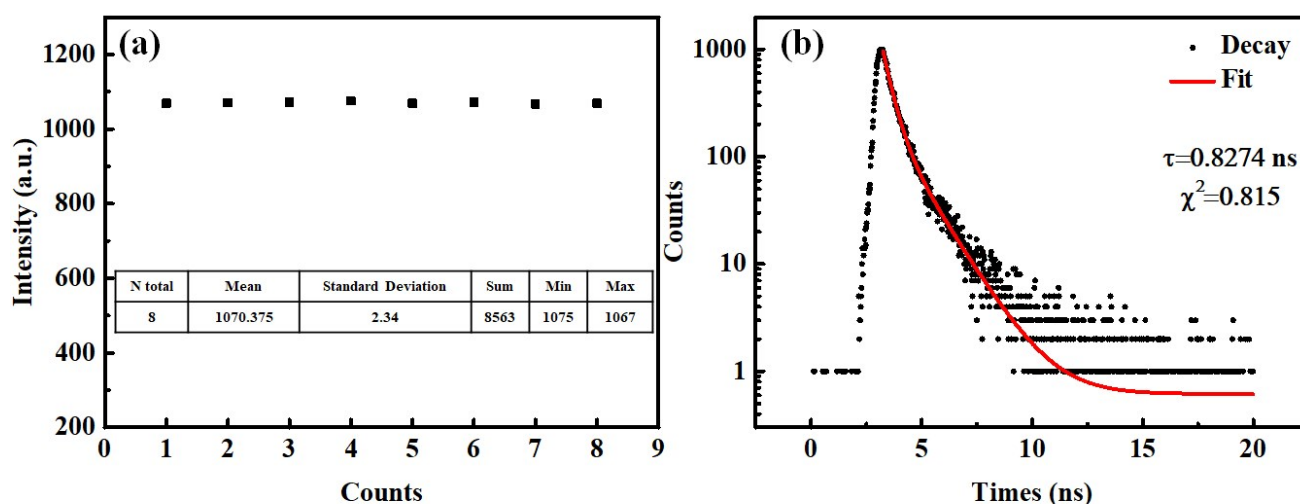


Figure S12. (a) Stability test of COP-108-S fluorescent probe. The corresponding limit of detection (LOD) was determined as 1.44 mM using the equation³ $\text{LOD} = 3 \times \text{S.D.} / K_{\text{sv}}$, where K_{sv} represents the slope of the Stern-Volmer plots, and S.D. is the standard deviation for the fluorescence intensity of COP-108-S in the absence of Hg^{2+} . (b) Fluorescence decay curve of COP-108-S dispersion in ethanol. The quenching rate constant $K_{\text{q}} = 5.9 \times 10^{12} \text{ mol s}^{-1}$ is calculated by the equation⁴ $K_{\text{sv}} = K_{\text{q}} \times \tau$. τ is the excited-state lifetime in the absence of analyte. When $K_{\text{q}} > 2.0 \times 10^{10} \text{ mol s}^{-1}$, the quenching process is the static quenching.⁵

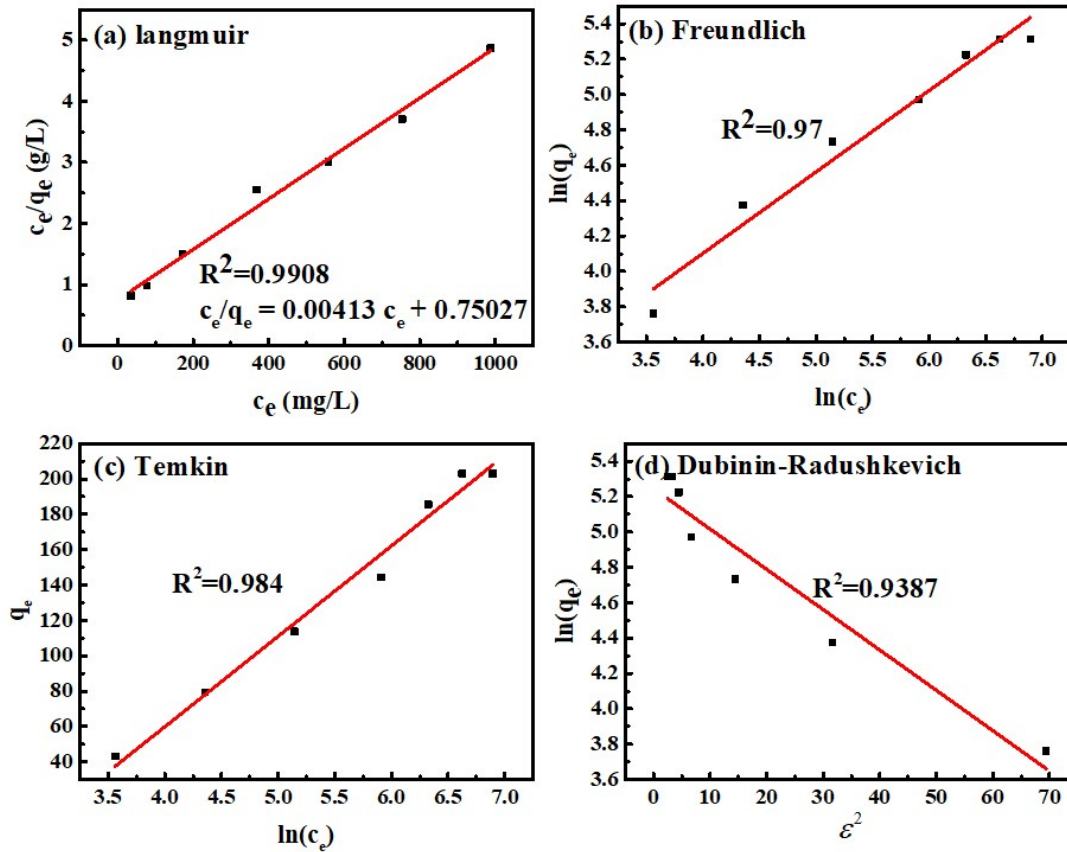


Figure S13. Plots of (a) Langmuir isotherm model, (b) Freundlich isotherm model, (c) Temkin isotherm model, (d) Dubinin-Radushkevich isotherm model for the adsorption of COP-108-S. The best linear correlation coefficient of Langmuir adsorption model, the equation⁶ is as follows:

$$\frac{C_e}{q_e} = \frac{C_e}{q_m} + \frac{1}{q_m K_L}$$

where q_m is the maximum adsorption capacity and K_L is Langmuir constant.

$$c_e/q_e=0.00413c_e+0.75027$$

$$q_m=240.96 \text{ mg g}^{-1}, K_L=0.006$$

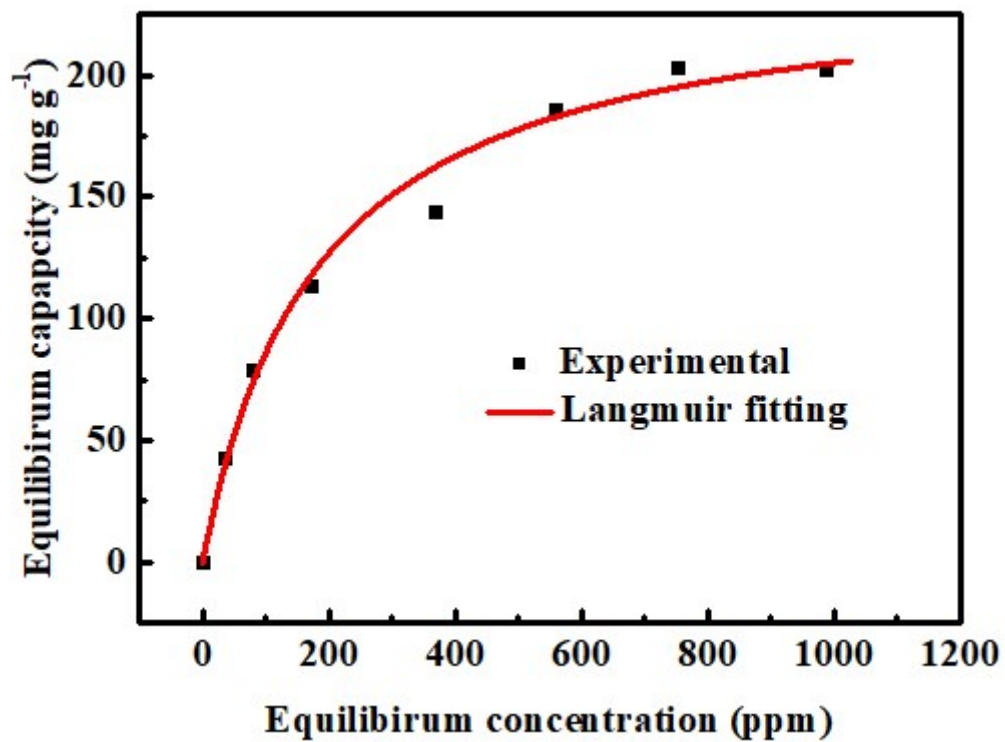


Figure S14. Equilibrium isotherms for Hg²⁺ adsorption on the polymers COP-108-S from aqueous solution (the lines were fitted by the Langmuir models).

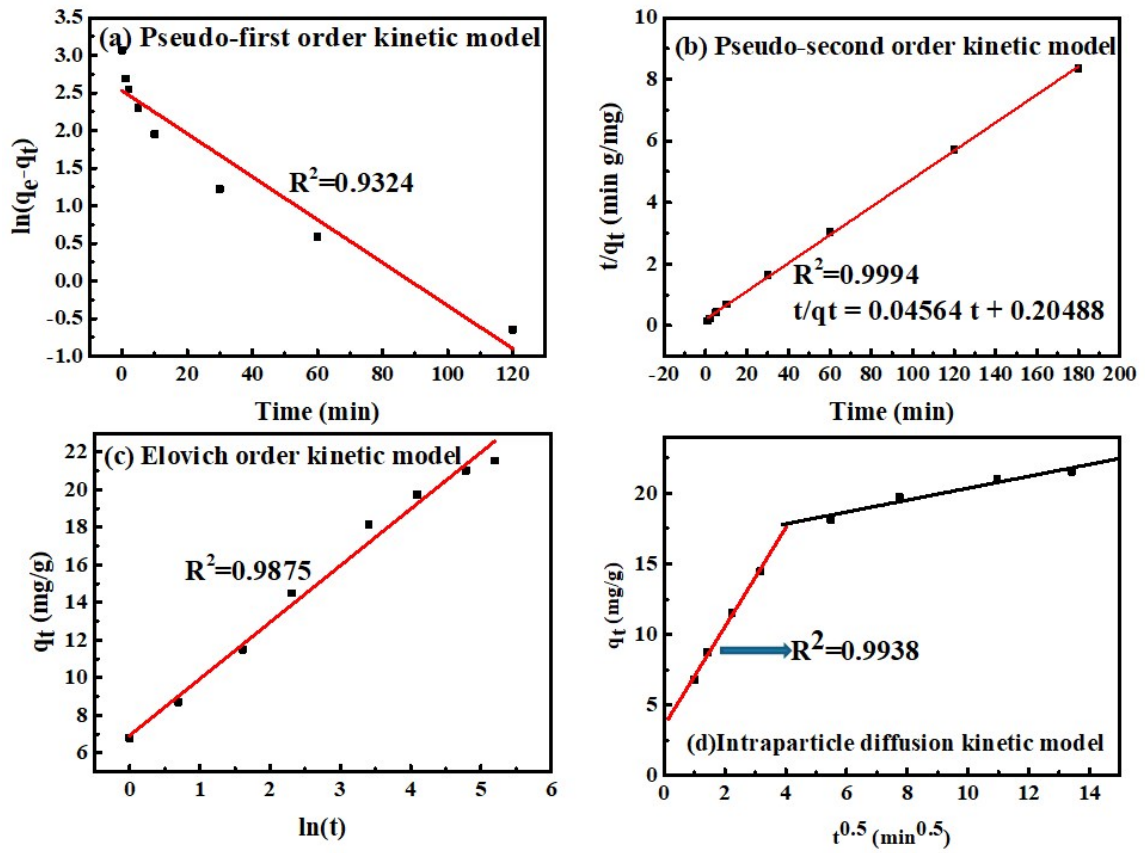


Figure S15. Kinetic adsorption simulation of Hg^{2+} on COP-108-S at a V/m ratio of 2000 mL g^{-1} . (a) Pseudo-first order kinetic model, (b) Pseudo-second-order kinetic model. (c) Elovich kinetic model kinetic model, (d) Intraparticle diffusion kinetic model. The best linear correlation coefficient of Pseudo-second-order kinetic model, the equation⁶ is as follows:

$$\frac{t}{q_t} = \frac{t}{q_e} + \frac{1}{k_2 q_e^2}$$

where k_2 are pseudo-second-order adsorption rate constants.

$$t/q_t = 0.04564t + 0.20488$$

$$q_e = 21.91 \text{ mg g}^{-1}, k_2 = 0.0107 \text{ g mg}^{-1} \text{ min}^{-1}$$

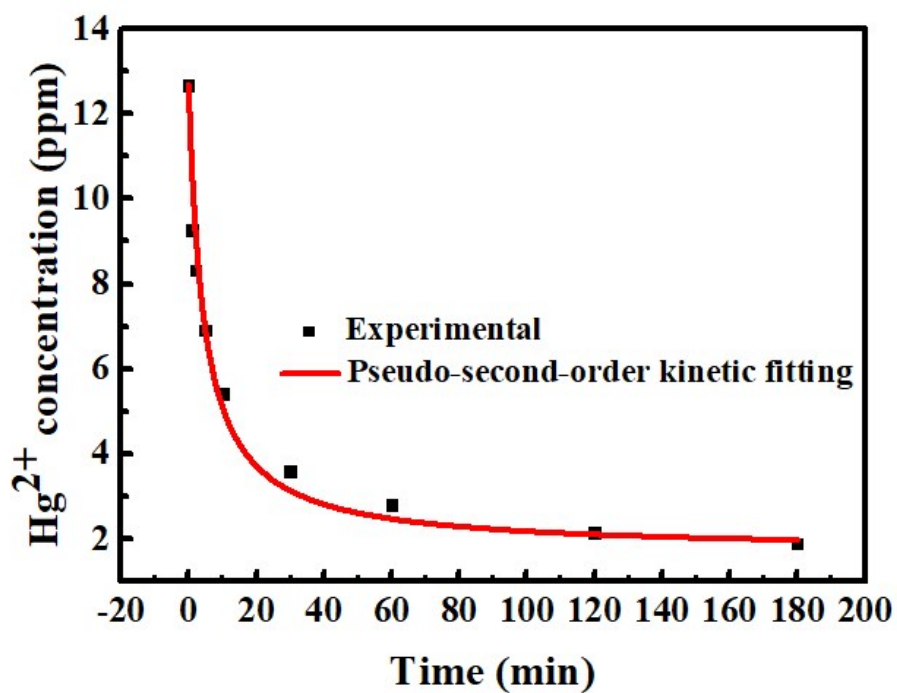


Figure S16. Kinetic adsorption of Hg²⁺ on COP-108-S. (the lines were fitted by the Pseudo-second-order kinetic).

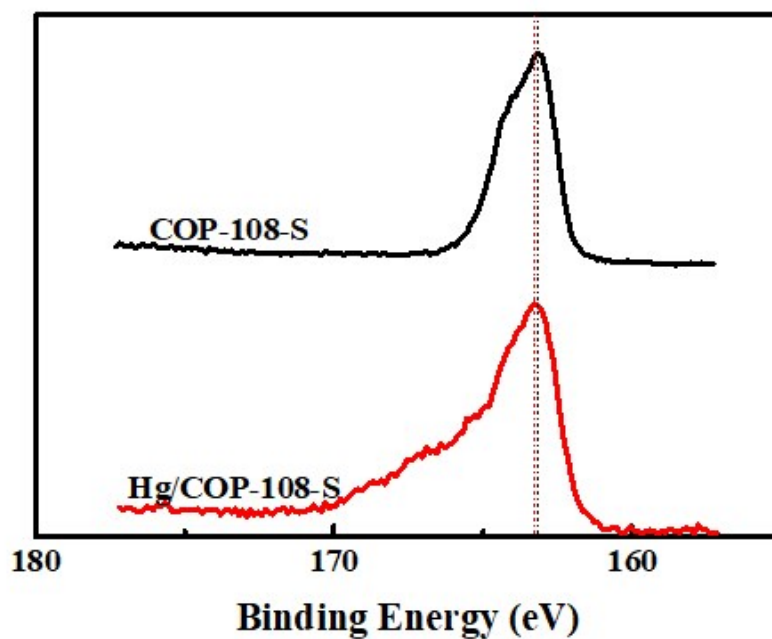


Figure S17. The XPS spectra of S 2p. The binding interactions between the Hg^{2+} and S species in Hg/COP-108-S were observed from the S 2p XPS spectra, which showed a **0.125 eV** shift for the S binding energy in Hg/COP-108-S compared to that of COP-108-S.

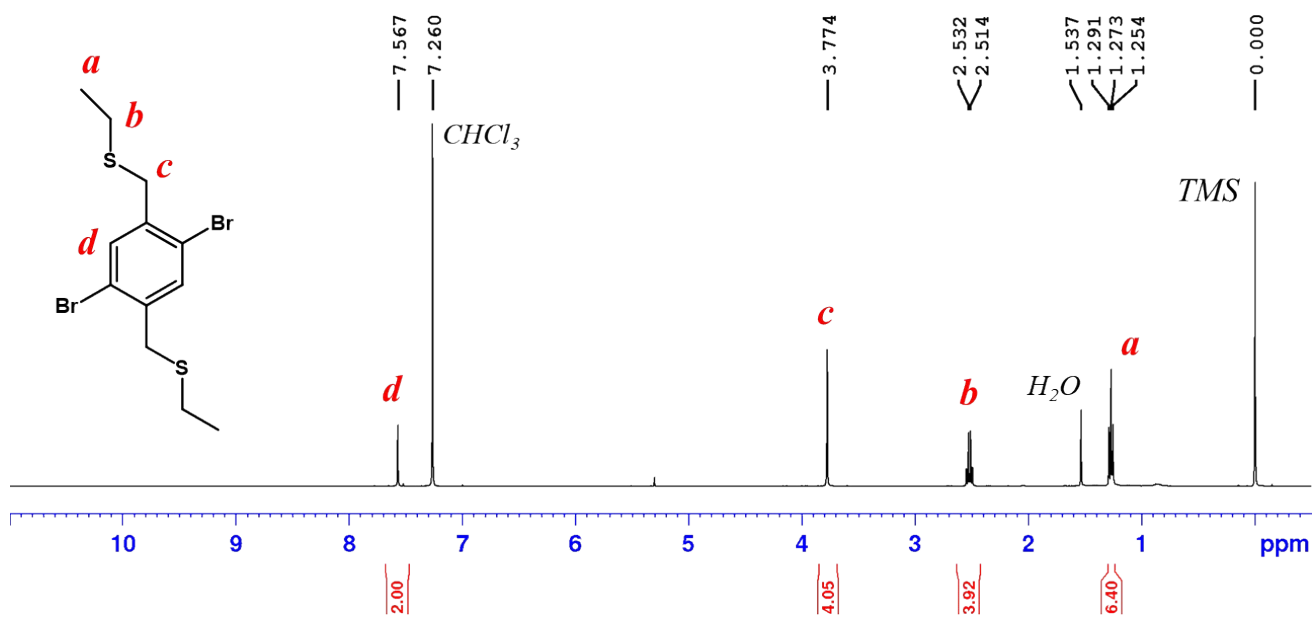


Figure S18. ¹H NMR spectrum of compound DB-S (400 MHz, CDCl₃, TMS, 298 K).

Section 4. Supporting References

- 1 S. Lu, Y. Hu, S. Wan, R. McCaffrey, Y. Jin, H. Gu and W. Zhang, Synthesis of Ultrafine and Highly Dispersed Metal Nanoparticles Confined in a Thioether-Containing Covalent Organic Framework and Their Catalytic Applications, *J. Am. Chem. Soc.*, 2017, **139**, 17082-17088.
- 2 Q. Sun, B. Aguila, J. Perman, L. D. Earl, C. W. Abney, Y. Cheng, H. Wei, N. Nguyen, L. Wojtas and S. Ma, Postsynthetically Modified Covalent Organic Frameworks for Efficient and Effective Mercury Removal, *J. Am. Chem. Soc.*, 2017, **139**, 2786-2793.
- 3 S. Y. Ding, M. Dong, Y. W. Wang, Y. T. Chen, H. Z. Wang, C. Y. Su and W. Wang, Thioether-Based Fluorescent Covalent Organic Framework for Selective Detection and Facile Removal of Mercury(II), *J. Am. Chem. Soc.*, 2016, **138**, 3031-7.
- 4 P. Das, G. Chakraborty and S. K. Mandal, Comprehensive Structural and Microscopic Characterization of an Azine-Triazine-Functionalized Highly Crystalline Covalent Organic Framework and Its Selective Detection of Dichloran and 4-Nitroaniline, *ACS Appl Mater Interfaces.*, 2020, **12**, 10224-10232.
- 5 Y. Tang, H. Huang, B. Peng, Y. Chang, Y. Li and C. Zhong, A thiadiazole-based covalent triazine framework nanosheet for highly selective and sensitive primary aromatic amine detection among various amines, *J. Mater. Chem. A.*, 2020, **8**, 16542-16550.
- 6 L. Lv, Y. Huang and D. Cao, Nitrogen-doped porous carbons with ultrahigh specific surface area as bifunctional materials for dye removal of wastewater and supercapacitors, *Appl. Surf. Sci.*, 2018, **456**, 184-194.